HHS Public Access

Author manuscript

Cell Signal. Author manuscript; available in PMC 2018 December 01.

Published in final edited form as:

Cell Signal. 2017 December ; 40: 133–142. doi:10.1016/j.cellsig.2017.09.008.

The C1 domain of Vav3, a novel potential therapeutic target

Jessica S. Kelsey, **Tamás Géczy**, **Christopher J. Kaler**, and **Peter M. Blumberg**[1]

Laboratory of Cancer Biology and Genetics, Center for Cancer Research, National Cancer Institute, NIH, Bethesda, MD 20892, U.S.A

Abstract

Vav1/2/3 comprise a protein family with guanyl nucleotide exchange activity for Rho and Rac as well as with motifs conferring adapter activity. Biologically, Vav1 plays a critical role in hematologic cell signaling, whereas Vav2/3 have a wider tissue distribution, but all 3 Vav proteins are implicated in cancer development. A structural feature of Vav1/2/3 is the presence of an atypical C1 domain, which possesses close structural homology to the typical C1 domains of protein kinase C but which fails to bind the second messenger diacylglycerol or the potent analogs, the phorbol esters. Previously, we have shown that five residues in the Vav1 C1 domain are responsible for its lack of phorbol ester binding. Here, we show that the lack of phorbol ester binding of Vav3 has a similar basis. We then explore the consequences of phorbol ester binding to a modified Vav3 in which the C1 domain has been altered to allow phorbol ester binding. We find both disruption of the guanyl nucleotide exchange activity of the modified Vav 3 as well as a shift in localization to the membrane upon phorbol ester treatment. This change in localization is associated with altered interactions with other signaling proteins. The studies provide a first step in assessing the potential for the design of custom C1 domain targeted molecules selective for the atypical C1 domains of Vav family proteins.

Keywords

phorbol ester; Rho GEF; signaling; membrane translocation

1. Introduction

C1 domains have emerged as a critical node in cellular signaling, conferring recognition of the lipophilic second messenger sn-1,2-diacylglycerol [1–4]. Diacylglycerol (DAG)[1] is generated downstream of numerous G-protein coupled receptors and receptor tyrosine kinases through the activation of phospholipase C in response to receptor triggering. While

[1]To whom correspondence should be addressed at: Peter M. Blumberg, Ph.D., Center for Cancer Research, National Cancer Institute, Building 37, Room 4048, 37 Convent Drive MSC4255, Bethesda, MD 20892-4255, U.S.A. blumberp@dc37a.nci.nih.gov; tel: 240-760-6632.

[1]Abbreviations: DAG, Diacylglycerol; PKC, Protein Kinase C; GEF, Guanine Nucleotide Exchange Factor; PMA, phorbol 12-myristate 13-acetate; PDBu, Phorbol 12,13-dibutyrate; CH domain, calponin homology domain; AD, Acidic domain; DH, Dbl homology; PH, Pleckstrin homology; SH3, Src homology 3; SH2, Src homology 2

protein kinase C family members are the best studied class of signaling proteins with DAG-responsive C1 domains [5,6] these domains are also present in the RasGRPs, which are guanyl exchange factors for Ras, in the chimaerins, which are GTPase activating proteins for Rac, in several members of the DAG kinase family, which provide negative feedback on DAG generation, and in the MRCK (myotonic dystrophy kinase-related Cdc42 -binding kinase), protein kinase D, and Munc-13 families [7,8].

In consequence of their central role in cellular signaling, PKC and the related classes of DAG-responsive proteins have been found to be prominently involved in cancer [7], diabetes [9], Alzheimer's disease [10], cardiovascular disease [11] and numerous other conditions [12–14]. Complementary therapeutic strategies have targeted both the catalytic activity and the C1 regulatory domain. Among C1 domain targeted compounds, ingenol mebutate (PEP005 or Picato™) has been approved by the FDA for actinic keratosis. Bryostatin 1 has been the subject of numerous clinical trials for cancer and is currently in clinical trial for Alzheimer's disease. Prostratin, bryostatin 1, and a range of other derivatives have proven of potential interest for sensitizing latent cells to drug therapy in HIV/AIDS [15].

Complementing the DAG-responsive C1 domains, which are referred to as "typical" C1 domains, are the "atypical" C1 domains, which possess sequence homology to the "typical" domains but fail to bind DAG or phorbol ester. We have shown that this latter classification can be further subdivided. The atypical C1 domains of PKCζ and PKCι [16] or of Vav1 [17] retain the binding cleft conformation of the typical domains but possess residues lining the rim of the binding cleft which interfere with ligand binding and membrane interaction. This contrasts with some other atypical C1 domains, such as that of Raf, which no longer maintain the binding cleft geometry [18].

A potential strategy for targeting those atypical C1 domains which retain the binding cleft geometry would be to use templates which fit in the binding cleft and which have substituents that can exploit interactions with the specific residues on the binding cleft rim that interfere with high affinity binding by DAG or related ligands. In the case of PKCζ/ι [16], the interfering residues are a series of 4 arginines. In Vav1 the interfering residues include a pair of glutamates. As an initial approach, we evaluated ligands for binding to the typical C1b domain of PKCδ into which we had introduced one or more of the interfering residues of the atypical domains. With such hybrid C1 domains, both in the case of PKCζ/ι [19] and Vav1 [17] we described DAG-lactones [20] with markedly improved selectivity compared to PDBu relative to that for the wild-type typical C1 domain. Although such compounds were not useful selective ligands for PKCζ/ι or Vav1, they provide initial support for the design strategy. Complementing our on-going efforts to develop the next generation of such compounds, in the present paper we explore the possible consequences of ligand interaction at the Vav3 atypical C1 domain. Our approach was to mutate the atypical C1 domain to permit phorbol ester binding and to then evaluate its functional consequences.

The three members of the Vav family, Vav1, Vav2, and Vav3 (Figure 1A), show marked structural and functional similarity. They possess two functional activities. First, they act as guanyl exchange factors for the Rac1 and Rho small GTPases. This function is mediated by the DH, PH, and C1 domains, under the negative regulation of the CH-AD region. Secondly,

they display adapter function through their SH3-SH2-SH3 domain [21]. Biologically, Vav1 is predominantly expressed in hematopoietic cells, although with frequent ectopic expression in neuroblastoma and pancreatic ductal adenocarcinoma [22], as well as in lung cancer and breast cancer [23]. In immune cells, it plays a central role in formation of the immunological synapse and, more generally, in remodeling of the actin cytoskeleton. Vav2/3 show more widespread tissue distribution than Vav1 [23] and have elevated expression in multiple tumor types, including oral squamous cell carcinoma, prostate cancer, colon cancer, and breast cancer. While structurally homologous to Vav1, Vav2/3 differ somewhat in their selectivity for Rho family isoforms, their ability to mobilize calcium, and their interaction partners [24,25].

Ligand interaction at the C1 domain of the Vav proteins might be expected to have two consequences. First, it would be predicted to inhibit the GEF activity of Vav. The C1 domain has been shown to be in contact with the DH domain, where it provides stabilization of the guanyl exchange activity [26], and disruption of the C1 domain has been shown to abrogate exchange and transforming activity [27,28]. Second, binding of a phorbol ester at the C1 domain would be expected to promote its membrane localization/stabilization. Indeed, we showed for Vav1 with a C1 domain mutated to bind phorbol ester that the addition of phorbol ester caused its translocation to the plasma membrane [17]. Necessarily, such membrane translocation would influence the interaction of Vav with those proteins binding to its adapter domain.

In the present study, we examined how similar Vav2 and Vav3 were to Vav1 in terms of the impact of the five critical residues identified as being responsible for the lack of DAG/phorbol ester binding of Vav1. We showed that they only partially accounted for the lack of binding activity of Vav2 but, for Vav3, their replacement could establish almost the same high binding affinity that we had previously described for Vav1. We then proceeded to characterize the effect of these mutations and phorbol ester on the GEF activity of Vav3, on its localization, and on select interacting partners. We confirm that phorbol ester binding disrupts Vav3 function and provides support for the possible impact of novel ligands designed to target the Vav3 atypical C1 domain.

2. Material and Methods

[20^{-3}H]Phorbol 12,13-dibutyrate ([^{3}H]PDBu) (17.2 Ci/mmol) was prepared as a custom synthesis by PerkinElmer Life Sciences (Boston, MA). PDBu and phorbol 12-myristate 13-acetate (PMA) were from LC Laboratories (Woburn, MA). LNCaP and PC3 human prostate cancer cells, fetal bovine serum (FBS), RPMI 1640 medium, and L-glutamine were obtained from the American Type Culture Collection (Manassas, VA). LB broth and LB agar plates used in bacterial culturing were purchased from K-D Medical, Inc. (Columbia, MD). Primers and oligos were from IDT (Integrated DNA Technologies, Coralville, IA).

2.1. Expression of GST-tagged Vav3 full length, C1 domains, and RhoA

The proteins were cloned into pGEX-5x-1 plasmids and expressed in DH5α competent cells (Invitrogen). The plasmids were then transformed into BL21 chemically competent cells (Invitrogen) for expression. The transformants were grown in LB broth at 37°C until an OD

of 0.5 was reached. Expression was induced with 0.5 mM IPTG. The cells expressing the C1 domains and RhoA were then incubated for 4 h at 37°C after which they were pelleted, while the cells expressing the full length Vav3 proteins were expressed by incubation overnight at room temperature before pelleting. Bacteria were lysed using pBER (Pierce) and the GST-tagged proteins were purified and eluted using a GST-spin column kit (Thermo Fisher Scientific). For GST-tagged bead preparations of RhoA proteins, the proteins were not eluted from the columns and the glutathione Sepharose with the GST-tagged proteins attached was collected from the columns. Full length Vav3 protein purification required the use of sarkosyl and was adapted from the protocols in Kae *et al.* [29] and Frangioni and Neel [30]. After induction of the cells, the pellet from a 500 ml culture of bacteria was resuspended in 10 ml STE buffer (10 mM Tris-HCl (pH 8.0), 1 mM EDTA, 150 mM NaCl). The cell suspension was treated with lysozyme (20 μg/ml, 30 min on ice), and 100 μl 1 M DTT and 1.4 ml 10% sarkosyl were then added. Cells were vortexed for 5 sec, then lysed by sonication (on ice, level 3, 2 × 10 sec). Lysates were cleared at 10,000 × g for 5 min. To the supernatant was added 4 ml 10% Triton X-100, followed by STE buffer to make a final volume of 20 ml. Glutathione Sepharose beads (GE Healthcare) were washed in the STE buffer and incubated with the lysate for 2 h at 4°C on a tumbler (500 μl beads to 10 ml lysate). The beads were washed three times in 1 × HK-LB (10 mM sodium phosphate (pH 7.2), 1% Triton X-100, 0.05% SDS, 10% glycerol, 150 mM NaCl, 10 mM $MgCl_2$, 1 mM EDTA and protease and phosphatase inhibitors). After washing the beads were resuspended to make a 50% slurry in 1 × HK-LB.

2.2. [^{3}H]PDBu binding assays

The dissociation constants (K_d values) of the Vav3 C1 domains were determined using the polyethylene glycol precipitation assay as described by Lewin and Blumberg [31].

2.3. F-actin staining

F-actin was stained with Acti-stain 555 (Cytoskeleton). Cells were fixed on cover slips at room temperature with 4% paraformaldehyde, washed in PBS, and permeabilized with 0.5% Triton X-100 for 5 min, then washed in PBS. The cells were stained with the Acti-stain (3.5μl/500 μl PBS) for 30 min, washed with PBS, and mounting media (Vector shield) was added.

2.4. Localization of GFP-tagged proteins

LNCaP cells and PC3 cells (between passage 3 and passage 20) were plated on Ibidi dishes (Ibidi, LLC) in RPMI 1640 medium containing 10% FBS and 2 mM L-glutamine and grown to 75% confluency at 37°C. Cells were transfected with GFP-tagged constructs using Xtreme gene reagent (Roche) per manufacturer's instructions. Experiments measuring translocation of the GFP-tagged constructs in response to addition of compounds to the cells were conducted 24 h after transfection, with images visualized using a 63×1.4 NA oil objective on Zeiss LSM 510 NLO, LSM 710 NLO or LSM 780 confocal microscopes (Carl Zeiss, Inc.). For excitation of GFP, the argon laser at 488 nm was used and the emission at 535–553 nm was determined. Processing of the images for translocation or localization was performed with the Zeiss software. Nuclear staining was with Hoechst 33342 (Life Technologies) at a concentration of 10 ng/ml in PBS for 15 min. For mCherry and F-actin

staining the 561 nm diode laser was used for excitation and filters of 490–534 nm were used for detecting emission. Imaging was carried out in the Confocal Microscopy Core Facility of the Center for Cancer Research.

2.5. Quantitation of Confocal Images

The Zeiss AIM software was used to obtain data. For GFP translocation to the membrane, in each experiment 6 regions of about 5 μm^2 were selected, with 3 overlying the cytoplasm and 3 overlying the plasma membrane, at 0, 5, 10, 30, and 45 min time points for each cell. Where indicated, cell images at 120 min were also analyzed. The average ratio of the mean intensity of the membrane/cytoplasm was determined for each time point. Values presented represent the mean ± SE of three independent experiments.

2.6. Statistical Analysis

Significance was determined with Graph Pad Prism 6 software, using the Student's t-test. A p-value < 0.05 was deemed significant.

2.7. Immunoprecipitation

Immunoprecipitation of GFP tagged proteins followed the standard immunoprecipitation protocol for SureBeads Magnetic Beads (Bio-Rad) with minor changes. Briefly, SureBeads were washed with PBS-T (PBS + 0.1% Tween 20) and then 4 μg anti-GFP antibody (Roche) was added and the beads were resuspended in binding buffer (0.05% NP-40, 20 mM Tris-HCl, pH 7.5, 300 mM KCl, 0.2 mM EDTA, 20% glycerol, 1 mM DTT, and protease inhibitors (cOmplete ULTRA tablets, Mini, EDTA, Roche, Indianapolis, IN) and phosphatase inhibitors (PhosSTOP, Roche, Indianapolis, IN)). The beads plus GFP antibody were incubated for 1 h at 4°C. The beads were then magnetized, the supernatant was discarded, and the beads washed 3 times in PBS-T. 200–500 μl of cell lysate in binding buffer at a concentration of about 3 mg/ml was added to the beads and incubated overnight at 4°C with rocking. The beads were magnetized and washed twice in wash buffer (0.01% NP-40, 20 mM Tris-HCl, pH 7.5, 300 mM NaCl, 0.2 mM EDTA, 20% glycerol, 0.5 mM DTT). Finally, the beads were resuspended on 60 μl protein loading buffer for Western blotting analysis.

2.8. Rho binding assays

GST-tagged full length RhoA protein was purified from bacterial cells and bound to glutathione Sepharose beads as previously described. LNCaP cells were transfected with GFP-tagged Vav3 proteins for 24–48 h and then lysed in binding buffer (0.05% NP-40, 20 mM Tris-HCl pH 7.5, 300 mM KCl, 0.2 mM EDTA, 20% glycerol, 1 mM DTT, and protease inhibitor (cOmplete ULTRA tablets, Mini, EDTA, Roche, Indianapolis, IN), cleared by centrifugation, and the lysate was incubated with purified RhoA-GST beads overnight at 4°C with rotation. Beads were washed 4 times with Wash buffer (0.01% NP-40, 20 mM Tris-HCl pH 7.5, 300 mM NaCl, 0.2 mM EDTA, 20% glycerol, 0.5 mM DTT) and resuspended in protein loading buffer. The amount of GFP, determined by immunoblotting, indicated the amount of GFP-tagged Vav3 bound to Rho.

2.9. GTPase activation assays

GTPase activation was assayed following the GTPase activation assay protocol from Cell BioLabs. Protease inhibitors (cOmplete ULTRA tablets, Mini, EDTA, Roche, Indianapolis, IN) and phosphatase inhibitors (PhosSTOP, Roche, Indianapolis, IN) were included in the lysis buffer. After the final binding step of the protocol, the beads were resuspended in protein loading buffer and the entire volume was subjected to immunoblotting to determine the amount of activated Rho.

2.10. Immunoblotting

Cell lysates were prepared and 15–22.5 μg of protein lysates (concentration determined using the Bio-Rad DC protein assay) (Bio-Rad, Hercules, CA) in SDS sample application buffer containing beta-mercaptoethanol were separated on Novex 10% Tris–glycine gels (Life Technologies, Grand Island, NY) and transferred to Whatman nitrocellulose membranes (Life Technologies, Grand Island, NY). The membranes were blocked with 5% nonfat dry milk (Bio-Rad, Hercules, CA) and incubated overnight with the primary antibody, washed with phosphate buffered saline containing 0.05% Tween 20, incubated for 1 h in the secondary antibody, and washed in phosphate buffered saline containing 0.05% Tween 20. The blots were developed by ECL (Bio-Rad), the signal detected on a Chemidoc touch imaging system (Bio-Rad), and the results analyzed with ImageLab 5.2.1 (Bio-Rad). The primary antibodies used were: monoclonal mouse β-actin, (Sigma, St. Louis, MO); pAKT (S473), Cell Signaling 4060S; AKT (pan), Cell Signaling (C67E7); EGFR(pan), Epitomics 1902-1; EGFR (pY1173), Epitomics (1124-1); Src, Cell Signaling (36D10); SALL2, Abcam (ab55723); PKCδ, Abcam (ab108972); Histone H3, Abcam (ab1791); Caveolin-1 (N-20), Santa Cruz (sc894); GFP, Roche. The secondary antibody was a horseradish peroxidase conjugated anti-rabbit (Bio-Rad, Hercules, CA) antibody. Immunoblot quantification was done using ImageJ, Gel analysis [32].

2.11. Measurement of interacting proteins

To identify interacting proteins, GFP-tagged Vav proteins were expressed in PC3 cells, lysates were prepared, and the lysates were subjected to immunoprecipitation as previously described. Proteins bound to the GFP-tagged Vav protein were measured by Western blotting for protein identification by antibody. The amount of protein on the Western blot was determined by ImageJ Gel analysis. The amount of total GFP in the sample was used for normalization between gels.

2.12 Molecular Modeling

To model the Vav3 C1 domain structure Pdb modeling files were generated using ITASSER and viewed with Swiss-Pdb viewer v4.1.0 [33–35]. The SwissDock program was utilized to illustrate docking of phorbol 13-acetate into the Vav3 5X C1 domain binding pocket by uploading the Vav3 5X C1 domain Pdb modeling file generated by ITASSER as the target selection and uploading the MOL2 file of phorbol 13-acetate as the ligand selection [36,37]. The MOL2 file for phorbol 13-acetate was generated by ChemDraw Prime 15.0 by uploading the SMILES for the compound.

3. Results

3.1. Phorbol ester binding by the Vav1/2/3 wild-type C1 domains and those substituted with residues from the corresponding positions of the PKCδ C1b domain

Geczy et al. [17] identified 5 key amino acid differences between the typical PKCδ C1b and Vav1 C1 domains that were responsible for the lack of sensitivity of the Vav1 C1 domain for phorbol ester (Figure 1B, highlighted residues). When the corresponding 5 amino acids of the PKCδ C1b domain were introduced into the Vav1 C1 domain, PDBu bound with a K_d value of 1.05 ± 0.14 nM, in contrast to no detectable binding by the WT Vav1 C1 domain [17]. Conversely, replacing these five amino acids in the C1 domain of PKCδ with the corresponding residues in the Vav1 C1 domain abolished detectable PDBu binding affinity. The five residues lined the rim of the phorbol ester binding pocket of the C1 domain, with three residues on the N-terminal loop (β1,2 loop) and two residues on the C-terminal loop (β3,4 loop). Mutating only the two amino acids on the C-terminal loop did not restore phorbol ester binding to the Vav1 domain. Mutating the three amino acids on the opposite side of the binding pocket, on the N-terminal loop, improved sensitivity to phorbol esters, but binding remained weak compared to the five amino acid mutations with a K_d value of 7330 ± 490 [17].

Vav2 and Vav3 share with Vav1 the two residues in the C-terminal loop that negatively affect phorbol ester binding by Vav1 (Figure 1B). In the N-terminal loop, Vav2 and Vav3 diverge from Vav1 in the triplet of residues found to interfere with phorbol ester binding by Vav1, with Vav3 showing a greater shift in the character of the substitutions. To explore how the residues in these five critical positions affected the phorbol ester sensitivity of Vav2 and Vav3, we prepared mutated versions of the Vav2 and Vav3 C1 domains incorporating combinations of the corresponding residues from the C1b domain of PKCδ (Figure 1C). Mutating all five key amino acids of the Vav2 C1 domain to the corresponding residues in the PKCδ C1b domain failed to confer potent phorbol ester binding activity such as had been found for Vav1 (Table 1). While measurable, the K_d of 650.7 ± 2.6 nM for the mutated Vav2 C1 domain remained three orders of magnitude weaker than that of the PKCδ C1b domain, indicating the presence of other important amino acids residues in the Vav2 C1 domain that interfere with phorbol ester binding. In contrast, when the five critical amino acids were mutated to the corresponding amino acids of the PKCδ C1b domain, the Vav3 C1 domain bound PDBu with a K_d of 4.7 ± 0.8 nM (Table 1). Mutating only the two key amino acids on the C-terminal loop in the C1 domain of Vav3 (designated the Vav3 2X mutant) resulted in a K_d for PDBu of 188 ± 35 nM, while mutating the three amino acids on the N-terminal loop (designated the Vav3 3X mutant) resulted in a K_d of 840 ± 120 nM. The recovery of at least moderate phorbol ester binding activity in the 2X mutant of Vav3, but not of Vav1 or Vav2, may reflect the greater adverse impact of the acidic residues in the 3X positions located at the tip of the N-terminal loop of the binding cleft in the C1 domains of Vav1 and Vav2. Given the greater phorbol ester binding activity of the mutated versions of Vav3 than of Vav2, we focused on Vav3 in our further experiments.

3.2. Analysis of membrane translocation of the mutant versions of full length Vav3 in response to phorbol ester treatment

To look at the response of the full length Vav3 and its 2X, 3X, and 5X mutants under physiological conditions, the constructs were tagged with GFP, expressed in LNCaP human prostate cancer cells, and membrane translocation in response to phorbol ester (10 μM PMA) was examined (Figure 2). Also examined were the constructs in which the CH and AD domains had been deleted from either wild-type Vav3 (designated Vav3 CaWT) or the 5X mutant (designated Vav3 Ca5X). Deletion of these domains generates constitutive guanyl nucleotide exchange activity [27]. As expected, neither the wild-type Vav3 nor the Vav3 CaWT translocated in response to the addition of PMA. Translocation of the Vav3 5X became visible after 10 min but became more evident after 2 h incubation with phorbol ester. The slow rate of translocation of the Vav3 5X was in marked contrast to the more rapid translocation observed previously for the Vav1 5X [17] and as observed here (Figure 2). For β2-chimaerin [38], RasGRP1 [39], and PKCβII [40] but not for Munc13 [41], the binding cleft of the C1 domain in the unliganded state is not solvent exposed. Rather, it is involved in intramolecular interactions which are necessarily lost when the C1 domain binds ligand and inserts into the lipid bilayer of the membrane. For Vav1 the C1 domain was shown to interact with the DH domain [26]. Presumably, for Vav3 this closed conformation is more stable than is the case for Vav1, leading to a slower response to the phorbol ester. In support of this interpretation, the Vav3 Ca5X, in which the first 176 amino acids constituting the inhibitory arm were removed from the Vav3 5X full length protein to yield a constitutively active protein, showed similar rapid kinetics of translocation as did the Vav1 5X and a similar or even greater extent of translocation. For these and other experiments, we chose a concentration of 10 μM PMA to get a maximal effect. Although such concentrations of PMA are often used, because of solubility issues the actual free concentration of PMA might be lower.

We also examined the translocation of the various constructs in a second cell type, the PC3 prostate cancer cell line, to determine whether the pattern of responses seen was unique to the LNCaP cells. In fact, the pattern of translocation in the PC3 prostate cancer cell line was largely similar to that seen in the LNCaP cells, except that the extent of translocation of the Vav3 5X reached the same extent as that of the Vav3 Ca5x by 2 h (Supplemental Figure 1).

3.3. Impact on GEF activity of the replacement of residues in the C1 domain of Vav3 to permit phorbol ester binding

3.3.1. Modeling predicts interference in GEF function—The crystallographic structure of the DH, PH, and C1 domains of Vav1, as well as modeling of the homologous Vav3, indicate that the 5 residues responsible for the lack of phorbol ester binding activity are close to the Vav1/3 GEF domains (DH and PH) (Figure 3A). In particular, the 2 residues of the C-terminal loop, when replaced with the corresponding residues of the PCKδ C1b domain, have the potential to cause interference [17], resulting from steric conflict for Leu24 and electrostatic interactions in the case of Lys26. A prediction therefore is that the mutated Vav3 may show reduced GEF activity. Additionally, modeling suggests that docking of phorbol ester into the C1 domain binding pocket of Vav3 5X will cause further interference (Figure 3B), since the side chains of the ligand extend upward into the alpha helices of the

DH domain. We therefore assessed both the effect of the altered residues in the mutated Vav3 on GEF activity as well as the further impact of phorbol ester addition.

3.3.2. Mutations in the C1 domain of Vav3 reduce interaction with Rho with further reduction in the presence of phorbol ester—We used a Rho-GST fusion protein bound to glutathione beads to assay the binding to Rho of Vav3 with either a wild-type or mutated C1 domain. The constitutively active (Ca) forms of Vav3 and its mutants were utilized since the inactive full length Vav3 showed little detectable Rho binding. GFP-tagged CaVav3 with the C1 domain WT and mutants 2X, 3X and 5X were transiently transfected in the LNCaP prostate cancer cell line. Cell lysates were incubated with Rho-GST beads in the absence of phorbol esters (DMSO) or with varying concentrations of phorbol esters. The CaVav3 with a WT C1 domain revealed full binding ability to Rho which was not altered by phorbol ester (Figure 4). All CaVav3 variants mutated in the C1 domain (2X, 3X and 5X) showed reduced Rho binding. The addition of phorbol ester led to a further reduction in Rho binding in the CaVav3 5X mutant. This result is consistent with the hypothesis that an appropriate ligand targeting the unmutated C1 domain of Vav3 might likewise disrupt the ability of Vav3 to interact with Rho.

3.3.3. Rho activation in response to CaVav3 is decreased for the CaVav3 variants mutated in the C1 domain—The above experiments explored the ability of the CaVav3 with wild-type and mutant C1 domains to bind to Rho. A complementary approach was to examine the ability of the CaVav3 with wild-type and mutant C1 domains to enhance Rho GTPase activity. Lysates were prepared from LNCaP cells expressing the full length and constitutively active CaVav3 with a wild-type C1 domain or the 5X mutant. Activated Rho could be separated from total Rho in the cell lysates by pull down with a bead-attached Rho binding domain that only recognizes the activated GTP-bound form of Rho. The CaVav3 wild-type protein was most efficient at activating Rho, which was expected since the CaVav3 has the inhibitory domain of Vav3 removed, liberating its guanyl exchange activity for Rho. As was described above for Rho binding activity, the CaVav3 with the five mutations in the C1 domain likewise showed diminished ability to activate Rho as compared to the CaWT version (Figure 5). Although the absolute levels of activation of Rho were substantially lower, the full length Vav3 (not constitutively active) with the five mutations in the C1 domain similarly showed reduced ability to activate Rho compared to the corresponding full length Vav3 (not constitutively active) with a wild-type C1 domain. Phorbol esters have been shown to cause a strong activation of Rho/Rac GTPases [42]. Any diminished Rho activation as a result of PMA binding to the Vav3 mutant could not be determined due to the strong activation of RhoA in the presence of phorbol ester.

A prominent effect of Rho activation is reorganization of the actin cytoskeleton. We therefore examined whether the mutations in the C1 domain of Vav3 led to a change in actin organization (Figure 6). LNCaP cells were transfected with either the GFP-tagged CaVav3 WT or the CaVav3 5x mutant. F-actin was stained with Acti-stain 555, yielding a red signal, and the CaVav3 transfected cells could be distinguished from the surrounding untransfected cells by the green signal from the GFP tag (Figure 6, an asterisk marks the GFP expressing cells). Both the CaVav3 WT and the CaVav3 5x mutant showed enhanced levels of actin

polymerization, but differences in the pattern of actin organization were evident, with the polymerized actin being more confined to the cell margins in the case of the CaVav3 5x and the cells being more rounded. We did not examine the additional effect of phorbol ester, since phorbol ester induced Rho/Rac GTPase activation has been implicated in the rearrangement of the actin cytoskeleton [42]. Thus, interpretation of a change in actin polymerization due to phorbol ester binding to the CaVav3 5x mutant would be obscured through the enhanced actin polymerization response caused by phorbol ester.

3.4. Phorbol ester modifies Vav3 5X adapter function in a fashion similar to that of Vav3 with a membrane targeting signal

The adapter region of Vav contributes to a rich pattern of protein interactions [25]. We wished to explore the possible impact of the mutations into the C1 domain of Vav3 at two levels. First, did the mutations affect protein-protein interactions? Second, did the translocation to membranes initiated by phorbol ester binding affect protein-protein interactions? PC3 cells were transfected with GFP-tagged Vav3 WT or 5X, treated in the absence or presence of phorbol ester, lysed, and proteins co-immunoprecipitated with the GFP-tagged Vav3 were detected. As controls for changes in localization, we included in parallel GPF-tagged Vav3 constructs into which either a myristylation signal to drive plasma membrane localization or a nuclear localization signal was incorporated (Supplementary Figure 2). Among possible interaction candidates, we focused on membrane associated proteins, since these seemed most likely to be affected by translocation of Vav3 5X in response to phorbol ester. In the absence of phorbol esters, Vav3 WT and Vav3 5X showed only a small and not significant difference in their ability to bind EGFR, PKCδ, and Src, implying that the mutations in the Vav3 C1 domain did not substantially interfere with these protein interactions (Figure 7). Addition of phorbol ester to the lysates caused significant increases in EGFR and PKCδ co-immunoprecipitated with the Vav3 5X as compared to the Vav3 WT. Similarly, enhanced co-immunoprecipitation was observed with the Vav3 construct tagged with the myristylation sequence to drive its plasma membrane association. While a similar trend was observed in the LNCaP cells, the results did not reach the level of statistical significance.

4. Discussion

Our understanding of C1 domains is surging, benefiting from the insights provided by multiple complementary approaches. We now appreciate that phorbol ester interaction in the binding cleft of the C1 domain represents a continuum from high affinity, through low affinity to no measurable affinity, and it finally extends to no affinity at all because of no binding cleft. Although classified as a “typical” C1 domain, the C1a domain of PKCθ was described as having an affinity for PDBu of >200 nM [43] and an affinity for DAG of 2000 nM, compared to 26 nM for the PKCθ C1b domain [44], and it did not contribute to PKCθ translocation (unpublished observations). Although classified as “atypical”, the C1 domain of RasGRP2 in fact bound PDBu with an affinity of 2,900 nM [45].

What can be the role of such C1 domains with low DAG/phorbol ester affinity? We now understand that even typical C1 domains are not simply hydrophobic switches, toggled by

DAG, but rather they typically toggle between two states, one engaged in intramolecular interactions to favor a closed protein conformation and the other interacting intermolecularly with DAG/phorbol ester and the lipid bilayer. While high affinity, typical C1 domains require an appropriate surface lining and surrounding the binding cleft for this latter, membrane bilayer associated state, C1 domains whose primary function is for intramolecular interactions may favor a different surface, such as the highly positively charged rim of the C1 domains of PKCζ/ι or the negatively charged rim of Vav1. Ligands appropriately functionalized to complement this surface have the potential for both specificity and selectivity.

DAG-lactones have proven to provide a powerful template for synthetically accessible, readily manipulated, high affinity ligands for the typical C1 domains [20]. Like the phorbol esters, they insert into the binding cleft of the C1 domain, both completing what in the typical C1 domains is a hydrophobic surface and providing side chains which can influence C1 domain interactions. For typical C1 domains such as those in PKC, the combination of the completed hydrophobic surface and the additional hydrophobicity contributed by the side chains drives insertion of the C1 domain into the lipid bilayer. Twin consequences are the translocation of PKC to the membrane and conformational change of the PKC, resulting both from loss of intramolecular interactions of the C1 domain as well as the new interactions with the membrane. Depending on the specific patterns of substitution, the DAG lactones can show quite diverse biological effects, which we have suggested reflect their localization of PKC to diverse membrane microdomains [46].

Our increasing understanding of C1 domains and their interaction with ligands has also begun to inform the design of ligands directed at atypical C1 domains. We have described a first generation of DAG lactones that have improved selectivity for the critical substitutions in the C1 domains of PKCζ/ι and of Vav1 which render these C1 domains atypical, although, as discussed, the binding of these DAG lactones was shown for C1 domains that did not have the full set of the critical residues distinguishing the C1 domains of PKCζ/ι and of Vav1 from those of typical C1 domains [17,19]. One obstacle in design is that, for typical C1 domains, one element of the pharmacophore is believed to be contributed by the phospholipid head groups in the membrane. Thus, modeling indicates that only one of the two carbonyls of the DAG-lactone (or DAG) is engaged in hydrogen bonding with the C1 domain [47], but both are required for high affinity binding [48]. To overcome this problem, an approach would be to recover this lost energy through additional interactions with the rim of the C1 domain. Depending on hydrophobicity, such a derivative could either simply occupy the Vav C1 domain binding cleft to disrupt the intramolecular interactions of the C1 domain or, as illustrated here with PMA, change the localization of Vav, altering its interactions with partners. Current collaborative efforts are underway to explore these possibilities.

Potentially, such DAG-lactones could be either stimulators, inhibitors, or simply modifiers of the pattern of activity. We have discussed elsewhere what such effects might be for PKCζ/ι [19]. For Vav family members, the evidence that their atypical C1 domains stabilize GEF activity would predict that an appropriately bulky ligand would inhibit GEF activity. This indeed was what we found with the Vav3 5X mutant upon addition of phorbol ester.

Such agents could have therapeutic utility for immune suppression and those cancers in which Vav isoforms are involved. We also showed that phorbol ester changed the pattern of interaction of Vav3 5X with interacting partners. Since we have shown that different C1 domain directed ligands can cause different patterns of localization of PKC isoforms, an expectation is that ligands could be designed with different modulatory effects.

"Atypical" C1 domains outnumber the typical C1 domains [1,17,49]. The biological importance of these proteins, such as is the case for PKCζ/ι and for the Vav family, our increasing ability to manipulate structures that interact with C1 domains, and our growing recognition of C1 domains as modules for protein-protein interactions rather than just for protein – lipid interactions, all make these interesting targets for drug development. The present paper represents one element of this effort, validating that the interposition of a ligand at the C1 binding cleft of Vav3 impacts its functional activity.

5. Conclusions

This study assesses a novel strategy for regulating the tumor promoting Vav proteins. Utilizing molecules that target the C1 domain of the Vav proteins would provide a way of regulating small GTPase activation and altering protein interactions, both of which could have implications in tumor development.

Acknowledgments

The research was supported by the Intramural Research Program of the National Institutes of Health, Center for Cancer Research, National Cancer Institute (Project Z1A BC 005270).

References

1. Hurley JH, Newton AC, Parker PJ, Blumberg PM, Nishizuka Y. Taxonomy and function of C1 protein kinase C homology domains. Protein Sci. 1997; 6:477–480. [PubMed: 9041654]
2. Colon-Gonzalez F, Kazanietz MG. C1 domains exposed: from diacylglycerol binding to protein interactions. Biochim Biophys Acta. 2006; 1761:827–837. [PubMed: 16861033]
3. Stahelin RV. Lipid binding domains: more than simple lipid effectors. J Lipid Res. 2009; 50:S299–S304. [PubMed: 19008549]
4. Das J, Rahman GM. C1 domains: structure and ligand-binding properties. Chem Rev. 2014; 114:12108–12131. [PubMed: 25375355]
5. Steinberg SF. Structural basis of protien kinase C isoform function. Physiol Rev. 2008; 88:1341–1378. [PubMed: 18923184]
6. Newton AC. Protein kinase C: poised to signal. Am J Physiol Endocrinol Metab. 2010; 298:E395–402. [PubMed: 19934406]
7. Griner EM, Kazanietz MG. Protein kinase C and other diacylglycerol effectors in cancer. Nat Rev Cancer. 2007; 7:281–294. [PubMed: 17384583]
8. Blumberg PM, Kedei N, Lewin NE, Yang D, Czifra G, Pu Y, Peach ML, Marquez VE. Wealth of opportunity. The C1 domain as a target for ddrug development. Curr Drug Targets. 2008; 9:641–652. [PubMed: 18691011]
9. Sobhia ME, Gerwal BK, Hata J, Rohit S, Punia V. Protein kinase C βII in diabetic complications: survey of structural, biological and computational studies. Exp Opin Ther Targets. 2012; 16:325–344.
10. Lucke-Wold BP, Turner RC, Logsdon AF, Simpkins JW, Alkon DL, Smith KE, Chen YW, Tan Z, Huber JS, Rosen CL. Common mechanisms of Alzheimer's disease and ischemic stroke: the role

of protein kinase C in the progression of age-related neurodegeneration. J Alzheimers Dis. 2015; 43:711–724. [PubMed: 25114088]

11. Ferreira JC, Brum PC, Mochly-Rosen D. βIIPKC and εPKC isozymes as potential pharmacological targets in cardiac hypertrophy and heart failure. J Mol Cell Cardiol. 2011; 51:479–484. [PubMed: 21035454]
12. McKernan LN, Momjian D, Kulkosky J. Protein kinase C: one pathway towards he eradication of latent HIV-1 reservoirs. Adv Virol. 2012; 2012:805347. [PubMed: 22500169]
13. Sobhia ME, Grewal BK, Paul ML, Patel J, Kaur A, Haokip T, Kokkula A. Protein kinase D inhibitors: a patent review (2010-present). Expert Opin Ther Pat. 2013; 23:1451–1468. [PubMed: 23795866]
14. Altman A, Kong KF. Protein kinase C inhibitors for immune disorders. Drug Discov Today. 2014; 19:1217–1221. [PubMed: 24892801]
15. Brogdon J, Ziani W, Wang X, Veazey RS, Xu H. In vitro effects of the small-molecule protein kinase C agonists on HIV latency reactivation. Sci Rep. 2016; 6:39032. [PubMed: 27941949]
16. Pu Y, Peach ML, Garfield SH, Wincovitch S, Marquez VE, Blumberg PM. Effects on ligand interaction and membrane translocation of the postively charged arginine residues situated along the C1 domain binding cleft in the atypical protein kinase C isoforms. J Biol Chem. 2006; 281:33773–33788. [PubMed: 16950780]
17. Geczy T, Peach ML, El Kazzouli S, Sigano DM, Kang JH, Valle CJ, Selezneva J, Woo W, Kedei N, Lewin NE, Garfield SH, Lim L, Mannan P, Marquez VE, Blumberg PM. Molecular basis for fairlure of “atypical” C1 domain of Vav1 to bind diacylglycerol/phorbol ester. J Biol Chem. 2012; 287:13137–13158. [PubMed: 22351766]
18. Mott HR, Carpenter JW, Zhong S, Ghosh S, Bell RM, Campbell SL. The solution structure of the Raf-1 cysteine-rich domain: a novel Ras and phospholipid binding site. Proc Natl Acad Sci USA. 1996; 93:8312–8317. [PubMed: 8710867]
19. Pu Y, Kang JH, Sigano DM, Peach ML, Lewin NE, Marquez VE, Blumberg PM. Diacylglycerol lactones targeting the structural features that idstinguish the atypical C1 domains of protein kinase C ζ and ι from typical C1 domains. J Med Chem. 2014; 57:3835–3844. [PubMed: 24684293]
20. Marquez VE, Blumberg PM. Synthetic diacylglycerols (DAG) and DAG-lactones as activators of protein kinase C (PK-C). Acc Chem Res. 2003; 36:434–443. [PubMed: 12809530]
21. Bustelo XR. Vav proteins, adaptors and cel signaling. Oncogene. 2001; 20:6372–6381. [PubMed: 11607839]
22. Katzav S. Vav1: a mematopoietic signal transcductionmolecule involved in human malignancies. Int J Biochem Cell Biol. 2009; 41:1245–1248. [PubMed: 19100858]
23. Katzav S. Vav1: a Dr. Jekyll and Mr. Hyde protein – good for the hematopoietic system, bad for cancer. Oncotarget. 2015; 6:28731–27742. [PubMed: 26353933]
24. Li SY, Du MJ, Wan YJ, Lan B, Liu YH, Yang Y, Zhang CZ, Cao Y. The N-terminal 20-amino acid region of guanine nucleotide exchange factor Vav1 plays a distinguished role in T cell receptor-mediated calcium signaling. J Biol Chem. 2013; 288:3777–3785. [PubMed: 23271736]
25. Bustelo XR. Vav family exchange factors: an integrated reglatory and functional view. Small GTPases. 2014; 5:2:1–12.
26. Rapley J, Tybulewicz VL, Rittinger K. Critical structural role for the PH and C1 domains of the Vav1 exchange factor. EMBO Rep. 2008; 9:655–661. [PubMed: 18511940]
27. Movilla N, Bustelo XR. Biological and regulatory properties of Vav-3, a new member of the Vav family of oncoproteins. Mol Cell Biol. 1999; 19:7870–7885. [PubMed: 10523675]
28. Zugaza JL, Lopez-Lago MA, Caloca MJ, Hosil M, Movilla N, Bustelo XR. Structural determinants for the biological activity of Vav proteins. J Biol Chem. 2002; 277:45377–45392. [PubMed: 12228230]
29. Kae H, Lim CJ, Spiegelman GB, Weeks G. Chemoattractant-induced Ras activation during Dictyostelium aggregation. EMBO Rep. 2004; 5:602–606. [PubMed: 15143344]
30. Frangioni JV, Neel BG. Solubilization and purification of enzymatically active glutathione S-transferase (pGEX) fusion proteins. Anal Biochem. 1993; 210:179–187. [PubMed: 8489015]
31. Lewin NE, Blumberg PM. [^{3}H]Phorbol 12,13-dibutyrate binding assay for protein kinase C and related proteins. Methods Mol Biol. 2003; 233:129–156. [PubMed: 12840504]

32. Rasband, WS. ImageJ. US National Institutes of Health; Bethesda, Maryland, USA: 1997–2014. http://imagej.nih.gov/ij/
33. Roy A, Kucukural A, Zhang Y. I-TASSER: a unified platform for automated protein structure and function prediction. Nat Protoc. 2010; 5(4):725–738. [PubMed: 20360767]
34. Zhang Y. I-TASSER server for protein 3D structure prediction. BMC Bioinformatics. 2008; 9:40. [PubMed: 18215316]
35. Guex N, Peitsch MC. SWISS-MODEL and the Swiss-PdbViewer: an environment for comparative protein modeling. Electrophoresis. 1997; 18:2714–2723. [PubMed: 9504803]
36. Grosdidier A, Zoete V, Michielin O. SwissDock, a protein-small molecule docking web service based on EADock DSS. Nucleic Acids Res. 2011; 39:W270–277. Web Server issue. [PubMed: 21624888]
37. Grosdidier A, Zoete V, Michielin O. Fast docking using the CHARMM force field with EADock DSS. J Comput Chem. 2011; 32:2149–2159. [PubMed: 21541955]
38. Canagarajah B, Leskow RC, Ho JY, Mischak H, Saidi LF, Kazanietz MG, Hurley JH. Structural mechanism for lipid activation of the Rac-specific GAP, beta2-chimaerin. Cell. 2004; 119:407–418. [PubMed: 15507211]
39. Iwig JS, Vercoulen Y, Das R, Barros T, Limnander A, Che Y, Pelton JG, Wemmer DE, Roose JP, Kuriyan J. Structural analysis of autoinhibitin in the Ras-specific exchange factor RasGRP1. eLife. 2013; 2:e00813. [PubMed: 23908768]
40. Leonard TA, Rozycki B, Saidi LF, Hummer G, Hurley JH. Crystal structure and allosteric activation of protein kinase C βII. Cell. 2011; 144:55–66. [PubMed: 21215369]
41. Xu J, Camacho M, Xu Y, Esser V, Liu X, Trimbuch T, Pan YZ, Ma C, Tomchick DR, Rosenmund C, Rizo J. Mechanistic insights into neurotransmitter release and presynaptic plasticity from the crystal structure of Munc13-1 C1C2 BMUN. Elife. 2017; 6:e22567. [PubMed: 28177287]
42. Xiao L, Eto M, Kazanietz MG. ROCK mediates phorbol ester-induced apoptosis in prostate cancer cells via p21Cip1 up-regulation and JNK. J Biol Chem. 2009; 284:29365–29375. [PubMed: 19667069]
43. Irie K, Nakahara A, Nakagawa Y, Ohigashi H, Shindo M, Fukuda H, Konishi H, Kikkawa U, Kashiwagi K, Saito N. Establishment of a binding assay for protein kinase C isozymes using synthetic C1 peptides and development of new medicinal leads with protein kinase C isozyme and C1 domain selectivity. Pharmacol Therap. 2002; 93:271–281. [PubMed: 12191619]
44. Melowic HR, Stahelin RV, Blatner NR, Tian W, Hayashi K, Altman A, Cho W. Mechanism of diacylglycerol-induced membrane targeting and activation of protein kinase C theta. J Biol Chem. 2007; 282:21467–21476. [PubMed: 17548359]
45. Czikora A, Lundberg DJ, Abramovitz A, Lewin NE, Kedei N, Peach ML, Zhou X, Merritt RC Jr, Craft EA, Braun DC, Blumberg PM. Stuctural basis for the failure of the C1 domain of Ras Guanine Necleotide releasing protein 2 (RasGRP2) to bind phorbol ester with high affinity. J Biol Chem. 2016; 291:11133–11147. [PubMed: 27022025]
46. Duan D, Sigano DM, Kelley JA, Lai CC, Lewin NE, Kedei N, Peach ML, Lee J, Abeyweera TP, Rotenberg SA, Kim H, Kim YH, El Kazzouli S, Chung JU, Young HA, Young MR, Baker A, Colburn NH, Haimovitz-Friedman A, Truman JP, Parrish DA, Deschamps JR, Perry NA, Surawski RJ, Blumberg PM, Marquez VE. Conformatinally constrained analogus of diacylglycerol. 29. Cells sort diacylglycerol-lactone chemical zip codes to produce diverse and selecctive biological activities. J Med Chem. 2008; 51:5198–5220. [PubMed: 18698758]
47. Nacro K, Bienfait B, Lee J, Han KC, Kang JH, Benzaria S, Lewin NE, Bhattacharyya DK, Blumberg PM, Marquez VE. Conformatinally constrained analogues of diacylglycerol (DAG).16. How much structural complexity is necessary for recognitin and high binding affinity to protien kinase C? J Med Chem. 2000; 43:921–944. [PubMed: 10715158]
48. Kang JH, Peach ML, Pu Y, Lewin NE, Nicklaus MC, Blumberg PM, Marquez VE. Conformationally constrined analogues of diacylglycerol (DAG). 25. Exploration of the sn-1 and sn-2 carbonyl functionality reveals the essential role fo the sn-1 carbonyl at the lipid interface in the binding of dAG-lactones to protein kinase C. J Med Chem. 2005; 48:5738–5748. [PubMed: 16134942]

49. Rahman GM, Das J. Modeling studies on the structural determinants for the DAG/phorbol ester binding to C1 domain. J Biomol Struct Dyn. 2015; 33:219–232. [PubMed: 24666138]

Highlights

- 5 key amino acid mutations result in phorbol ester sensitivity in the atypical Vav3 C1 domain.
- Phorbol ester binding to the Vav3 C1 domain disrupts guanyl nucleotide exchange activity.
- A change in Vav3 localization is induced by phorbol ester binding.
- The change in localization alters protein interactions.

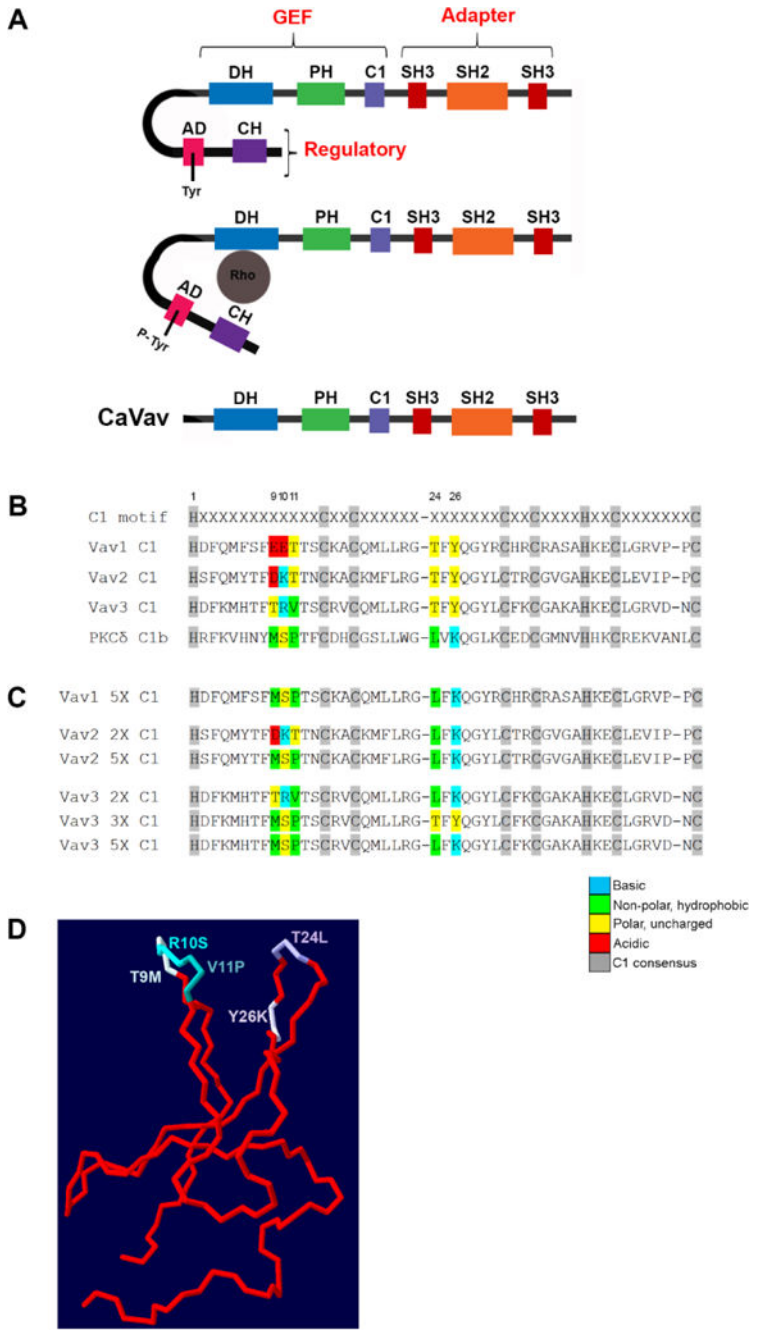

Figure 1. Vav protein structure

A) The domain structure of Vav1/2/3. The GEF activity of Vav is subject to autoinhibition by the AD and CH domains, which can be relieved either by tyrosine phosphorylation of the AD domain or experimentally in constructs by deletion of these domains. CH, calponin homology; AD, Acidic domain; DH, Dbl homology; PH, Pleckstrin homology; C1, C1 domain; SH3, Src homology 3; SH2, Src homology 2. B) Amino acid sequence alignment of the Vav isoform C1 domains and comparison with the PKCδ C1b domain. Amino acid residues subjected to mutational analysis are highlighted in color. Residues forming the defining C1 consensus are highlighted in grey. C) Amino acid sequences of the mutated

Vav1/2/3 C1 domains. D) 3D Structure of the Vav3 C1 domain, showing the location of the mutated residues. Pdb files were constructed using ITASSER [33,34] and proteins modeled utilizing the SwissDock Pdb-viewer [35].

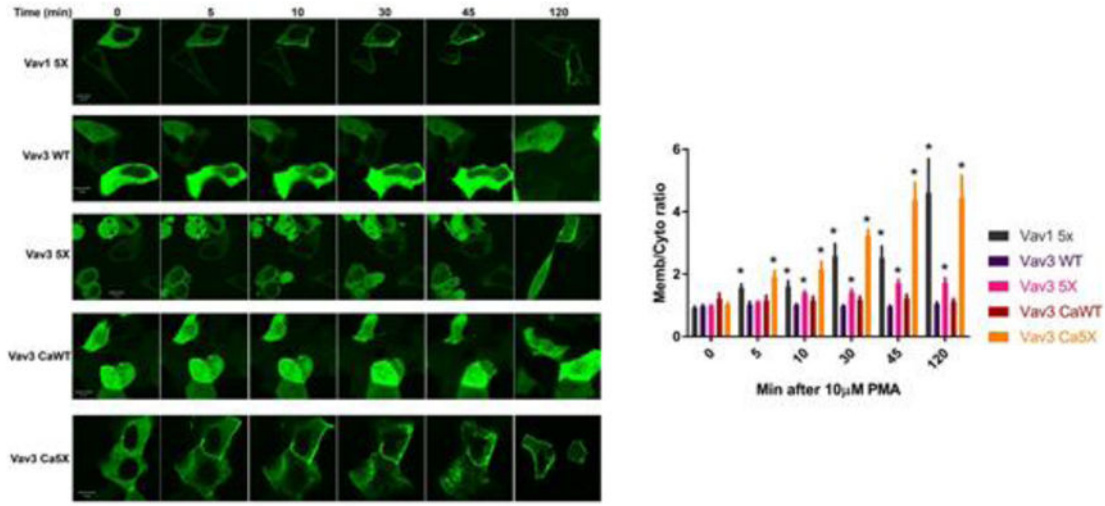

Figure 2. Translocation of full length Vav1/3 with a wild-type or mutant C1 domain in response to phorbol ester treatment of LNCaP cells

A) LNCaP cells expressing the GFP-tagged full length Vav1 and Vav3 wild-type and the indicated Vav3 mutant constructs were treated with 10 μM PMA and then imaged by confocal microscopy at the indicated time points (min). At least 3 independent experiments were performed under each condition and representative series of images are displayed. B) The translocation of the GFP-tagged protein from cytoplasm to membrane was quantitated and expressed as the ratio of the GFP-tagged protein in the membrane to that in the cytoplasm at the indicated time points. Values represent the mean ± SEM derived from at least 3 cells in each of at least 3 independent experiments. '*' indicates significant difference ($p < 0.05$) from Vav3 WT.

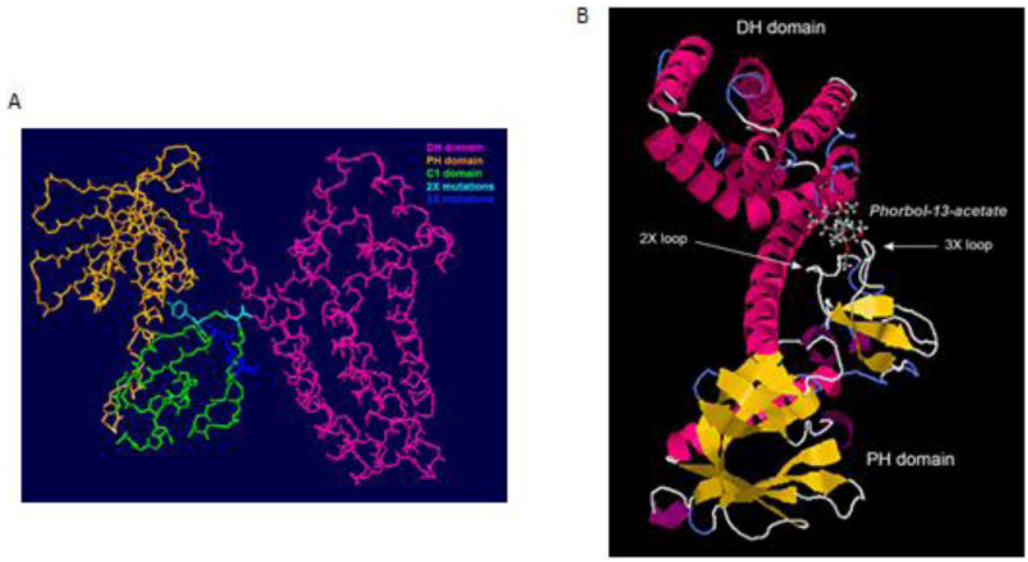

Figure 3. Modeling the 5X mutations in the Vav3 C1 domain binding pocket

A) Modeling the Vav3 5X C1 domain with the mutated 2x and 3x residues color coded to indicate their localization relative to the DH and PH domains. Their proximity to the GEF domain is evident. The Swiss Pdb viewer software was used [35]. B) Docking of phorbol 13-acetate into the binding pocket. The phorbol ester is located in the Vav3 5X C1 domain binding pocket and the potential interference between the side chains of the phorbol ester and the Vav DH domain is illustrated. The SwissDock program was utilized [36,37].

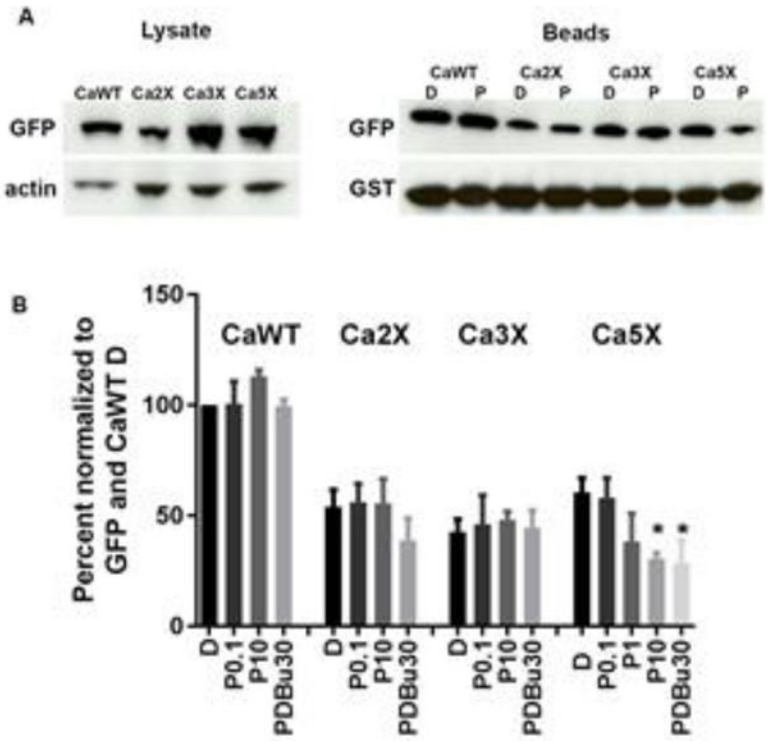

Figure 4. Binding of Rho by Vav3 wild-type and its C1 domain mutants in the absence and presence of phorbol ester

The ability of the constitutively active (Ca) Vav3 and its C1 domain mutants to bind Rho was determined. GFP-tagged CaVav3 with wild-type or mutant C1 domains was expressed in LNCaP cells. Cell lysates were prepared and incubated in the absence or presence of phorbol ester at the indicated concentrations and binding to Rho-GST beads was then measured. A) Representative immunoblots showing expression of GFP-tagged CaVav3 wild-type and C1 domain mutants in total lysate (left) and their binding to Rho-GST beads (right). D, DMSO; P, PMA 10 μM. B) Quantification of the binding of the GFP-tagged CaVav3 wild-type and C1 domain mutants to the Rho-GST beads (note more extensive range of ligand conditions). D, DMSO; P0.1, 0.1 μM PMA; P1, 1 μM PMA; P10, 10 μM PMA; PDBu30, 30 μM PDBu. Values represent the mean ± SEM from 3 independent experiments (P1 value, from 2 experiments) and are normalized to that of the DMSO control for CaWT. '*' indicates significant difference ($p < 0.05$) from the DMSO control.

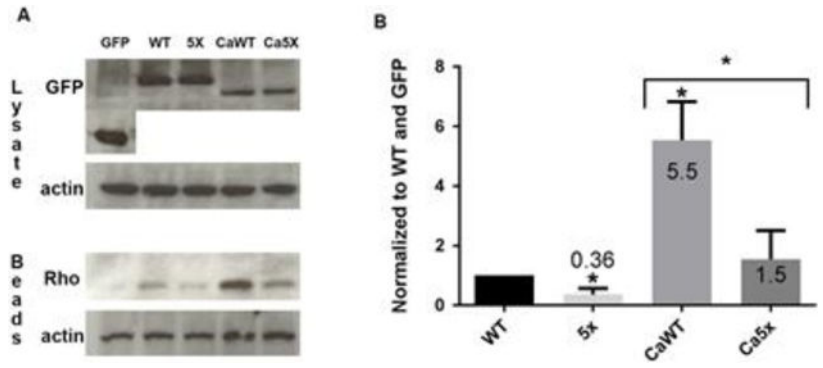

Figure 5. Activation of Rho by Vav3 wild-type and its C1 domain mutants

The level of active Rho was assayed by its binding to the Rho binding domain (RBD) immobilized on beads. The Rho binding domain will only recognize and allow pull down of the activated GTP-bound form of Rho. LNCaP cells were transfected with GFP as a control and with the full-length and constitutively active (Ca) forms of GFP-tagged Vav3 with either a WT or 5X mutant C1 domain. Cell lysates were prepared and incubated with the RBD beads. A) Representative immunoblots showing the level of GFP-tagged protein expression (top) and the amount of Rho protein being pulled down by the RBD beads (bottom). B) Blots were scanned and quantitated. Values represent the mean ± SEM from 3 independent experiments. '*' indicates significant difference ($p < 0.05$) for comparisons of Vav3 WT versus WT5X, WT versus CaWT, and CaWT versus Ca5X.

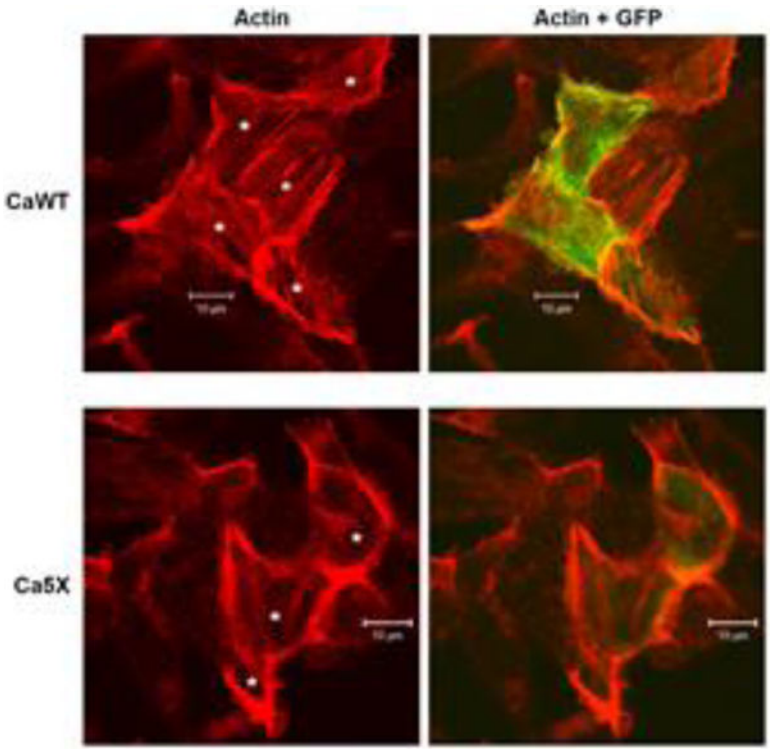

Figure 6. Differences in F-actin cytoskeletal organization between CaWT and Ca5X expressing cells

LNCaP cells transiently transfected with GFP-tagged CaWT and Ca5X constructs (green) were stained for F-actin (Red) and imaged by confocal microscopy. The GFP signal appears faint in some cells when overlaid with the actin staining, so cells expressing the GFP-tagged proteins CaWT (top) and Ca5X (bottom) are indicated by asterisks in the actin only images. Note the more intense F-actin staining in the transfected cells and the lesser F-actin staining in the interior of the Ca5X expressing cells.

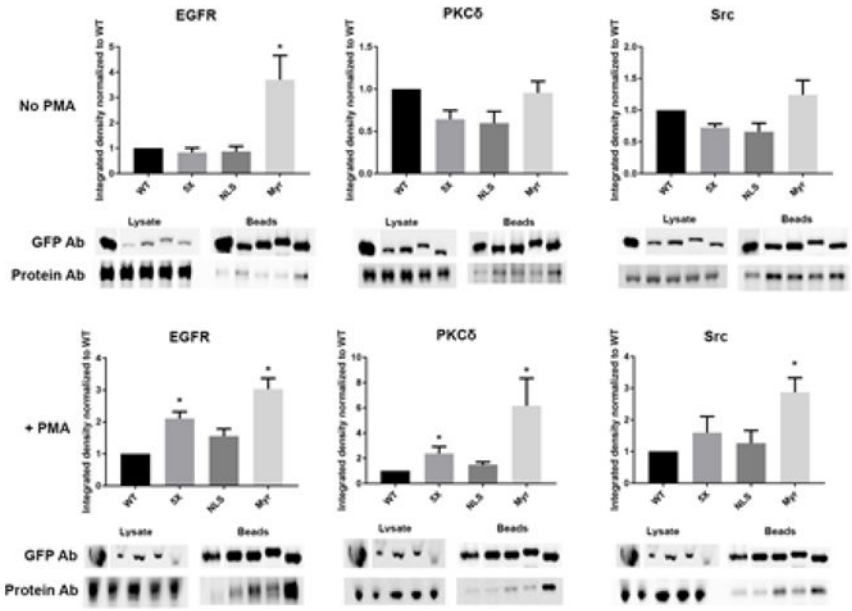

Figure 7. Co-immunoprecipitation of interacting partners with the GFP-tagged Vav3 WT, 5X mutant, and Vav3 localization mutants in the presence and absence of PMA

PC3 cells were incubated for 1 h in the presence of 10 μM PMA (top) or without PMA (bottom). Lysates were prepared and subjected to immunoprecipitation with anti-GFP antibody. The GFP-tagged Vav3 protein and the indicated co-precipitated interacting proteins were detected by immunoblotting. For each interaction a representative immunoblot is displayed showing the GFP signal of the Vav3 protein in the upper panel and the specific protein of interest (as indicated above the graphs) in the lower panel. The graphs show the mean ± SEM from at least 3 replicate immunoprecipitations and western blots. An (*) signifies significant difference ($p < 0.05$) relative to WT Vav3. WT, wild-type Vav3; 5X, Vav3 5X; NLS, nuclear localization signal tagged Vav3; Myr, myristylation site tagged Vav3.

Table 1

Binding affinities of [^{3}H]PDBu to Vav1/2/3 wild-type and mutant C1 domains.

Vav1 C1	**K_d(nM)**	**Relative to PKCδ C1b**
WT	NA	NA
2X (T24L/Y26K)	NA	NA
3X (E9M/E10S/T11P)	7330 ±490	38,000 ×
5X (E9M/E10S/T11P/T24L/Y26K)	1.05 ± 0.14	5.4×
Vav2 C1	**K_d(nM)**	**Relative to PKCδ C1b**
WT	NA	NA
2X (T24L/Y26K)	NA	NA
5X (D9M/K10S/T11P/T24L/Y26K)	650.7 ± 2.6	3370 ×
Vav3 C1	**K_d(nM)**	**Relative to PKCδ C1b**
WT	NA	NA
2X (T24L/Y26K)	188 ± 35	938 ×
3X (T9M/R10S/V11P)	840 ± 120	4380 ×
5X (T9M/R10S/V11P/T24L/Y26K)	4.7± 0.8	23.5×

GST-tagged C1 domains were expressed in bacteria, purified, and their binding affinities for [^{3}H]PDBu determined. Values, mean ± SEM of triplicate experiments except for Vav3 3X, for which only 2 replicates were performed. NA, no activity. Values for Vav1 are from Geczy *et al.* [17].